Biochimica et Biophysica Acta, 1023 (1990) 168–183
Elsevier

BBAMEM 74781

Vanadate-catalyzed, conformationally specific photocleavage of the Ca^{2+}-ATPase of sarcoplasmic reticulum

Miklos Vegh *, Elek Molnar ** and Anthony Martonosi

Department of Biochemistry and Molecular Biology, State University of New York, Health Science Center at Syracuse, Syracuse, NY (U.S.A.)

(Received 6 October 1989)

Key words: ATPase, Ca^{2+}-; Calcium ion dependence; Photocleavage; Vanadate; Antibody; Sarcoplasmic reticulum

Vanadate-sensitized photocleavage of the Ca^{2+}-ATPase of rabbit sarcoplasmic reticulum was observed upon illumination of sarcoplasmic reticulum vesicles or the purified Ca^{2+}-ATPase by ultraviolet light in the presence of 1 mM monovanadate or decavanadate. The site of the photocleavage is influenced by the Ca^{2+} concentration of the medium. When the [Ca^{2+}] is maintained below 10 nM by EGTA, the vanadate-catalyzed photocleavage yields fragments of ≅ 87 and ≅ 22 kDa, while in the presence of 2–20 mM Ca, polypeptides of 71 and 38 kDa are obtained as the principal cleavage products. These observations indicate that the site of the vanadate-catalyzed photocleavage is altered by changes in the conformation of Ca^{2+}-ATPase. Selective tryptic proteolysis, at Arg-505-Ala-506, combined with covalent labeling of Lys-515 by fluorescein 5′-isothiocyanate and with the use of anti-ATPase antibodies of defined specificity, permitted the tentative allocation of the sites of photocleavage to the A fragment near the T_2 cleavage site in the absence of Ca^{2+}, and to the B fragment between Lys-515 and Asp-659 in the presence of 2–20 mM Ca^{2+}. The loss of ATPase activity during illumination is accelerated by calcium in the presence of vanadate. The vanadate-catalyzed photocleavage in the presence of Ca^{2+} is consistent with the existence of an ATPase-Ca^{2+}-vanadate complex (Markus et al. (1989) Biochemistry 28, 793–799).

Introduction

The structural analysis of the Ca^{2+} transport ATPase of sarcoplasmic reticulum was significantly aided by the specific cleavage of the Ca^{2+}-ATPase into well-defined fragments by trypsin [1–8], chymotrypsin [9], pepsin [10], thermolysin [10], cyanogen bromide [11,12] and HBr [13].

The amino acid sequence data derived from these studies, together with sequence data deduced from cDNA sequences [14–19] permitted the tentative assignment of certain functional sites (ATP binding, phosphorylation, Ca^{2+} binding) to predicted structural domains within the ATPase molecule [20–22]. These assignments are currently analyzed by site-specific mutagenesis and other techniques [23–26].

The primary cleavage of the rabbit fast isoenzyme of Ca^{2+}-ATPase by trypsin (T_1) occurs at Arg-505-Ala-506, yielding two large fragments, A and B, with apparent molecular masses of ≅ 57 and ≅ 52 kDa, respectively [1–3]. The T_1 cleavage site is near the reactive Lys-515 that can be selectively labeled with fluorescein 5′-isothiocyanate [27], permitting ready identification of the B fragment by fluorescence. The A and B fragments are held together by secondary forces [28], with preservation of the ATPase activity and Ca^{2+} transport [29]. The rate of tryptic cleavage at the T_1 site is rapid, whether the enzyme is stabilized in the E_1 state by Ca^{2+}, or in the E_2V state by EGTA and vanadate [30,31]. Species differences in the structure or isoenzyme composition of Ca^{2+}-ATPases are indicated by the observations that in lobster [32,33] and carp Ca^{2+}-ATPase [34], the primary tryptic cleavage occurs at a different

* On leave from the 2nd Institute of Biochemistry, Semmelweis University Medical School, H-1444 Budapest, Hungary.
** On leave from the Institute of Biochemistry, Albert Szent-Gyorgyi University Medical School, H-6701 Szeged, Hungary.

Abbreviations: SR, sarcoplasmic reticulum; Ca^{2+}-ATPase, Ca^{2+}, Mg^{2+}-activated ATP phosphohydrolase of sarcoplasmic reticulum (EC 3.6.1.38); T_1-Ca^{2+}-ATPase, Ca^{2+}-ATPase cleaved with trypsin at the T_1 site; SDS, sodium dodecylsulfate; PBS, phosphate-buffered saline; HRP, horseradish peroxidase; Hepes, *N*′-2-hydroxyethylpiperazine-*N*′-2-ethanesulfonic acid; EGTA, ethyleneglycol bis(β-aminoethyl ether)-*N,N,N′,N′*-tetraacetic acid; AMP-PNP, 5′-adenylyl imidodiphosphate (p[NH]ppA).

Correspondence: A.N. Martonosi, Department of Biochemistry, SUNY, Health Science Center at Syracuse, Syracuse, NY 13210, U.S.A.

site, yielding an 85 kDa and a 20 kDa fragment. Slight differences were also observed between the size of the cleavage fragments obtained from the fast skeletal muscle Ca^{2+}-ATPase and from the slow Ca^{2+}-ATPase isoenzymes of slow-twitch skeletal, cardiac and smooth muscles [35].

The secondary tryptic cleavage site (T_2) of the rabbit sarcoplasmic reticulum Ca^{2+}-ATPase is in the A fragment between Arg-198 and Ala-199, yielding an A_1 fragment of $\cong 34$ kDa and an A_2 fragment of $\cong 23$ kDa, with some loss of enzymatic activity [29]. The T_2 cleavage is highly sensitive to the conformation of the Ca^{2+}-ATPase and proceeds at a rapid rate only in the presence of Ca^{2+} (E_1 state), but it is completely blocked in the presence of EGTA and vanadate [30,36].

Vanadate-catalyzed photolytic cleavage and modification of the polypeptide chain was observed in several phosphohydrolases, such as dynein [37–39], myosin [40,41] and a microtubule associated ATPase [42,43]. Although the mechanism of vanadate action is unknown, it is suspected that vanadate acts as an analogue of inorganic phosphate [44,45]. The target of vanadate-catalyzed photolysis is assumed to be an aromatic amino acid near the binding site for inorganic phosphate or vanadate [40,41,46,47].

Here we report the vanadate-catalyzed photocleavage of the Ca^{2+}-ATPase of sarcoplasmic reticulum, that yields distinct cleavage products in the presence and absence of Ca^{2+}, suggesting the existence of two distinct cleavage sites that are selectively exposed, depending on the conformation of the Ca^{2+}-ATPase.

Experimental Procedures

Materials

The sources of chemicals were as follows: sodium metavanadate, sodium dodecylsulfate, and 2-mercaptoethanol from Fisher Scientific Co., Rochester, NY 14624, U.S.A.; NADH, phospho*enol*pyruvate, EGTA, glutathione (reduced), AMP, AMP-PNP, ATP, uric acid, pyruvate kinase, lactate dehydrogenase, superoxide dismutase, catalase, horseradish peroxidase, trypsin, soybean trypsin inhibitor, bilirubin, α-tocopherol, β-carotene, leupeptin, sodium deoxycholate, anti-mouse and anti-rabbit IgG conjugated with horseradish peroxidase, antifoam A, thimerosal, 4-chloro-1-naphthol, and Stains-All from Sigma Chemical Corp., St. Louis, MO 63178, U.S.A.; FITC from Molecular Probes, Inc., Eugene, OR 97402, U.S.A.; A23187 and Amido black 10-B from Calbiochem-Behring Diagnostics, La Jolla, CA 92112, U.S.A.; glycylglycine from Aldrich Chemical Co., Milwaukee, WI 53233, U.S.A., and nitrocellulose sheets from Bio-Rad Inc., Richmond, CA 94804, U.S.A.

Methods

Skeletal muscle sarcoplasmic reticulum vesicles. Skeletal muscle sarcoplasmic reticulum vesicles were isolated from predominantly white skeletal muscles of the rabbit according to Nakamura et al. [48] and stored until use at $-70\,^{\circ}C$ in a medium of 0.3 M sucrose, 10 mM Tris-maleate (pH 7.0) at a protein concentration of 30–40 mg/ml [49]. Before starting the experiments the vesicles were washed with 9 volumes of a medium containing 0.1 M KCl, 20 mM Hepes-K^+, 5 mM $MgCl_2$ (pH 7). This medium (basic medium) was used in all experiments for ultraviolet illumination. In several experiments the sarcoplasmic reticulum preparations were further purified by deoxycholate extraction [50,51] to obtain purified Ca^{2+}-ATPase preparations. The final pellet was resuspended in basic medium and either used immediately or stored at $-70\,^{\circ}C$ at a protein concentration of 40–60 mg/ml.

Tryptic proteolysis of Ca^{2+}-ATPase; preparation of the A and B tryptic fragments. Tryptic digestion of sarcoplasmic reticulum proteins was carried out essentially as described by Dux and Martonosi [36] and Dux et al. [30,31], utilizing the observation that vanadate permits the cleavage of Ca^{2+}-ATPase at the T_1 cleavage site into the A and B fragments, but inhibits the subsequent cleavage at the T_2 site into smaller subfragments. The purified Ca^{2+}-ATPase preparations were resuspended at a protein concentration of 2 mg/ml in basic medium, supplemented with 1 mM EGTA, and either monovanadate or decavanadate (1 mM each) at $25\,^{\circ}C$. The digestion was started by the addition of trypsin (50 μg/ml) and stopped 15 min later by the addition of 200 μg/ml soybean trypsin inhibitor. The digest was centrifuged at $105\,000 \times g$ for 45 min at $2\,^{\circ}C$, and the pellet was washed once with the original volume of basic medium, supplemented with 1 mM EGTA and 50 μg/ml trypsin inhibitor. After centrifugation ($105\,000 \times g$, 45 min, $2\,^{\circ}C$), the final pellet was resuspended in basic medium containing 1 mM EGTA, and used for further experiments.

Protein concentration was measured according to Lowry et al. [52].

Preparation of 'monovanadate' and 'decavanadate' stock solutions. Stock solutions of 50 mM vanadate were prepared by boiling Na_3VO_3 at pH 10 in water for 15 min. 'Monovanadate' stock solutions were adjusted to pH 7 by stepwise addition of HCl and boiled for 10 min to minimize their decavanadate content. In addition to monovanadate these solutions contain oligovanadates in concentrations determined by the final vanadate concentration [53]. Stock solutions containing primarily the decavanadate polyanion were prepared by adjusting the pH of 50 mM vanadate solutions with HCl below pH 4 and storing the solution overnight or longer at $4\,^{\circ}C$. The final pH was adjusted to 7 directly before the experiment was started [53].

Labeling of Ca^{2+}-ATPase and its tryptic fragments with fluorescein 5′-isothiocyanate (FITC). The covalent labeling of Ca^{2+}-ATPase with FITC was carried out

either before or after ultraviolet illumination. Samples containing sarcoplasmic reticulum vesicles, the purified Ca^{2+}-ATPase, or its proteolytic subfragments were suspended in basic medium at a protein concentration of 2–2.5 mg/ml. The pH was adjusted to 8.1 and the EGTA concentration to 1 mM for samples labeled before ultraviolet illumination, or to 3 mM for samples labeled after illumination. The difference in EGTA concentration was necessary to compensate for differences in Ca^{2+} concentration between the two sets of samples. An ethanolic solution of FITC was added to the samples to a final concentration of 7 nmol/mg protein, and the reaction was allowed to proceed at 25 °C for 30 min in the dark. For ultraviolet illumination after labeling, the pH of the samples was adjusted with 0.3 M HCl to pH 7.0. Samples labeled after UV illumination were applied directly for SDS-polyacrylamide gel electrophoresis.

Photosensitized cleavage of Ca^{2+}-ATPase. Illumination was performed with a Mineralight UV lamp (type R-52, Ultra-Violet Products, Inc., San Gabriel, CA, U.S.A.) supplied with filter (No. 62376). The emission of this lamp consists of three main lines with maxima at 253, 309 and 363 nm, with approximate intensity ratios of $\lambda_1 : \lambda_2 : \lambda_3 = 5.6 : 1 : 1.1$. The total radiation intensity was $\cong 70$, 11 and 2.8 $mW \cdot cm^{-2}$, for samples at 2, 5 and 10 cm distance from the lamp, respectively.

Samples (0.2– ml) were placed in cuvettes of 1 cm^2 surface area and illuminated from 2, 5 or 10 cm distance at 2 °C with horizontal, circular shaking at 1 cycle/s. The samples contained 2 mg protein/ml, in a medium of 0.1 M KCl, 20 mM Hepes-K^+, 5 mM $MgCl_2$ (pH 7), supplemented with EGTA, $CaCl_2$, mono- or decavanadate, and other additions, as described in the figure legends. Temperature was controlled by a Tele-Thermometer (model 43TD, Yellow Springs Instrument Co., Inc., Yellow Springs, OH, U.S.A.). Changing the temperature to 28 °C did not result in significant change of the cleavage patterns.

ATPase activities. ATPase activities were measured essentially as described by Varga et al. [49] using a coupled enzyme assay at 25 °C in a medium of 0.1 M KCl, 20 mM Tris-HCl, 5 mM $MgCl_2$, 0.45 mM $CaCl_2$, 0.5 mM EGTA, 5 mM ATP, 0.42 mM phospho*enol*-pyruvate, 0.42 mM NADH, 7.5 IU/ml pyruvate kinase, 18 IU/ml lactate dehydrogenase, and 1 μM A23187 at pH 7.4. Final sarcoplasmic reticulum protein concentration in the assay was 5 μg/ml.

p-Nitrophenyl phosphate hydrolysis. *p*-Nitrophenyl phosphate hydrolysis was measured at 25 °C by recording the changes in absorbance at 420 nm caused by the liberation of *p*-nitrophenol [49,54]. The basic medium supplemented with 0.1 mM $CaCl_2$, 1 μM A23187, and 4.7 mM *p*-nitrophenyl phosphate served as assay medium. Protein concentration was 50 μg/ml. For ATPase and *p*-nitrophenyl phosphatase activity measurements the sarcoplasmic reticulum vesicles were preincubated with Ca^{2+} in the assay medium at 25 °C for 5 min, before the addition of substrate.

^{51}V-NMR spectroscopy. Spectra were recorded at 25 °C at a vanadium frequency of 94.69 MHz on a Bruker WM 360 WB spectrometer with a pulse Fourier-transform NMR technique as described by Csermely et al. [53]. Sarcoplasmic reticulum vesicles (2 mg protein/ml) were suspended in basic medium (0.1 M KCl, 20 mM Hepes-K^+, 5 mM $MgCl_2$), supplemented with EGTA and vanadate (1 mM each) in the absence or presence of 2 mM $CaCl_2$.

SDS-polyacrylamide gel electrophoresis and Western blots. SDS-polyacrylamide gel electrophoresis was carried out as described earlier [30,31,36]. Samples taken for electrophoresis were diluted with 0.4 volume of sample buffer containing 10% sodium dodecylsulfate, 20 mM Tris-HCl (pH 8.0), 2% β-mercaptoethanol, 20% glycerol and 0.2% Bromophenol blue. After incubation for 10 min at 100 °C, aliquots containing 30–100 μg protein were applied for gel electrophoresis. Electrophoresis was performed essentially according to Laemmli [55] using 6–18% polyacrylamide gradient gels. Phosphorylase *b* (94 kDa), bovine serum albumin (67 kDa), ovalbumin 43 kDa), carbonic anhydrase (30 kDa), soybean trypsin inhibitor (20 kDa) and α-lactalbumin (14 kDa) were used as molecular weight markers (Pharmacia, Piscataway, NJ 08854, U.S.A.). Fluorescent bands on gels were photographed using ultraviolet light for excitation and yellow filters for the isolation of scattered exciting light from the emitted fluorescence. Proteins were stained with Coomassie blue. The gel patterns were evaluated by densitometry on an LKB Ultroscan laser densitometer (model 2202) connected with a Hewlett-Packard (model 3390A) integrator-plotter.

Occasional staining with Stains-All was performed as described by King and Morrison [56]. The procedure of Schibeci and Martonosi [57] was used to remove the sodium dodecylsulfate from gels before staining.

Electrophoretic transfer for immunoblot analysis of sarcoplasmic reticulum proteins. After SDS-polyacrylamide gel electrophoresis, the proteins were transferred to nitrocellulose sheets (Bio-Rad 14 × 18 cm, 0.45 μm pore size) using an LKB Transphor-electroblotting unit. The transfer buffer contained 10 mM imidazole, 30 mM glycylglycine, 0.1% sodium dodecylsulfate, and 20% methanol (pH 8.3). The transfer required 3 hours at 40 V, and a temperature of 10–15 °C.

For localization of proteins the nitrocellulose sheets were stained with 0.2% (w/v) Amido black for 5 min in 45% methanol, 10% acetic acid solution and then destained in 25% methanol, 5% acetic acid.

Immunostaining of nitrocellulose membranes. After the electrophoretic transfer, the nitrocellulose sheets were immersed in a solution of 5% (w/v) nonfat dry milk,

0.01% Antifoam A, and 0.0001% merthiolate in a phosphate-buffered saline (PBS) solution containing 1.5 mM KH_2PO_4, 8.1 mM Na_2HPO_4, 0.137 M NaCl and 2.7 mM KCl, for 2 h [58]. The sheets were then incubated for 2 h with a 1 : 1000 dilution of the various antisera in phosphate-buffered saline, containing 1% milk powder at room temperature. After washing twice for 5 min with phosphate-buffered saline containing 0.05% Tween 20, and once with phosphate-buffered saline containing 1% milk powder, the membrane filters were incubated for 2 h at room temperature with horseradish-peroxidase conjugated anti-mouse or anti-rabbit IgG (Sigma Chemical Co., St. Louis, MO 63178, U.S.A.) diluted to 1 : 1000 in phosphate-buffered saline containing 1% milk powder. The reaction was terminated by washing the sheets twice for 5 min each with phosphate-buffered saline containing 0.05% Tween 20 and once with a solution of 0.9% NaCl and 10 mM Tris (pH 7.4). The bound, conjugated IgG was visualized by reaction for ≅ 15 min with a solution containing 10 ml 0.9% NaCl, 10 mM Tris (pH 7.4), 1 ml of 0.3% 4-chloro-1-naphthol in methanol and 0.01 ml of 30% (v/v) H_2O_2. When bands became visible, the nitrocellulose filters were rinsed with distilled water, photographed and dried at room temperature for subsequent analysis.

Enzyme-linked immunoadsorbent assay (ELISA). Sarcoplasmic reticulum proteins (0.03, 0.1, 0.3 and 1 μg) were dispersed in 100 μl coating buffer (13 mM sodium carbonate, 35 mM sodium bicarbonate (pH 9.6)) and immobilized in polyvinyl chloride microtiter wells (Bio-Rad), at 4°C for 12 h [59]. The plates were washed three times for 3 min each with washing buffer containing 0.05% Tween 20 in phosphate-buffered saline (PBS) (pH 7.2). 100-μl aliquots of 1% solution of bovine serum albumin in PBS were added to each well and incubated for 1 h at room temperature. The plates were then reacted with a 1 : 1000 dilution of the A52 monoclonal antibody for 1 h at room temperature, followed by washing the wells with the washing buffer. The bound monoclonal antibody was reacted with an anti-mouse antibody horseradish peroxidase (HRP) conjugate (1 : 1000 dilution) for 1 h at room temperature. Finally, the plates were rinsed and reacted for 30 min with a substrate solution containing 67 mM dibasic sodium phosphate, 35 mM citric acid, pH 5.0, 0.08% *o*-phenylenediamine and 0.03% H_2O_2 to form a colored product for spectroscopy. The reaction was terminated with 50 μl of 2 M sulfuric acid, and the absorbance was determined at 405 nm with a Titertek Multiskan microtitration plate photometer (No. 78504) produced by Flow Laboratories, Inc., McLean, VA 22102, U.S.A.

Characterization of the anti-Ca^{2+}-ATPase antibodies. Monoclonal antibodies against the Ca^{2+}-transport ATPase of sarcoplasmic reticulum were kindly provided by Dr. David H. MacLennan, Banting and Best Department of Medical Research, Charles H. Best Institute, University of Toronto, Toronto, Ontario, Canada (antibody A52) and by Dr. Douglas M. Fambrough, Department of Biology, Johns Hopkins University, Baltimore, Maryland (antibody 7C6). The antigenic site for antibody A52 [60] was determined to be in the region of amino acids 659 and 668 in the sequence of the fast isoenzyme of the Ca^{2+}-ATPase, corresponding to the B tryptic peptide (MacLennan, D.H., personal communication). The antigenic site for antibody 7C6 is in the A_1 tryptic fragment of the fast isoenzyme of Ca^{2+}-ATPase (Fambrough, D.M., personal communication). Both localizations were confirmed in the present studies. In addition, a polyclonal rabbit, anti-rat Ca^{2+}-ATPase antibody with preferential specificity against the A_2 tryptic fragment of the Ca^{2+}-ATPase was also used [61].

Results

Vanadate-catalyzed photocleavage of sarcoplasmic reticulum Ca^{2+}-ATPase

Ultraviolet light illumination of sarcoplasmic reticulum vesicles in the presence of monovanadate or decavanadate leads to the fragmentation of Ca^{2+}-ATPase. The time course of monovanadate-sensitized cleavage is illustrated in Fig. 1. The cleavage pattern is influenced by Ca^{2+}. When Ca^{2+} ions are chelated with EGTA, the photocleavage occurs at the V cleavage site and fragments with approximate molecular masses of 87 kDa (fragment V_1) and 22 kDa (fragment V_2) are formed. When the vanadate-catalyzed photocleavage is performed in the presence of 20 mM $CaCl_2$, the cleavage occurs at a distinct VC cleavage site and fragments of 71 kDa (fragment VC_1) and 38 kDa (fragment VC_2) can be observed. There was no photocleavage during illumination in the absence of vanadate.

Fragmentation seems to be faster in the presence of Ca^{2+}. The formation of VC_1 can be observed already after 15 min of illumination and within 60 min a significant portion (about half) of the Ca^{2+}-ATPase was cleaved to yield the VC_1 and VC_2 fragments. The VC_2 fragment forms a slightly diffuse band indicating some inhomogeneity. In the absence of Ca^{2+} the rate of photocleavage is slower, and the apparent molecular weight of the V_1 and V_2 fragments is better defined.

In addition to the photocleavage, ultraviolet irradiation of sarcoplasmic reticulum with or without vanadate caused crosslinking and aggregation of sarcoplasmic reticulum proteins. The aggregates did not readily dissociate in sodium dodecylsulfate and were retained on the surface of the electrophoresis gel. The amount of aggregated material increased with the length of exposure to light, making it impractical to demonstrate greater than ≅ 40–60% cleavage of the Ca^{2+}-ATPase.

The products of the photocleavage originate from the Ca^{2+}-ATPase, because there was no significant change in the amounts of calsequestrin and the 160 kDa pro-

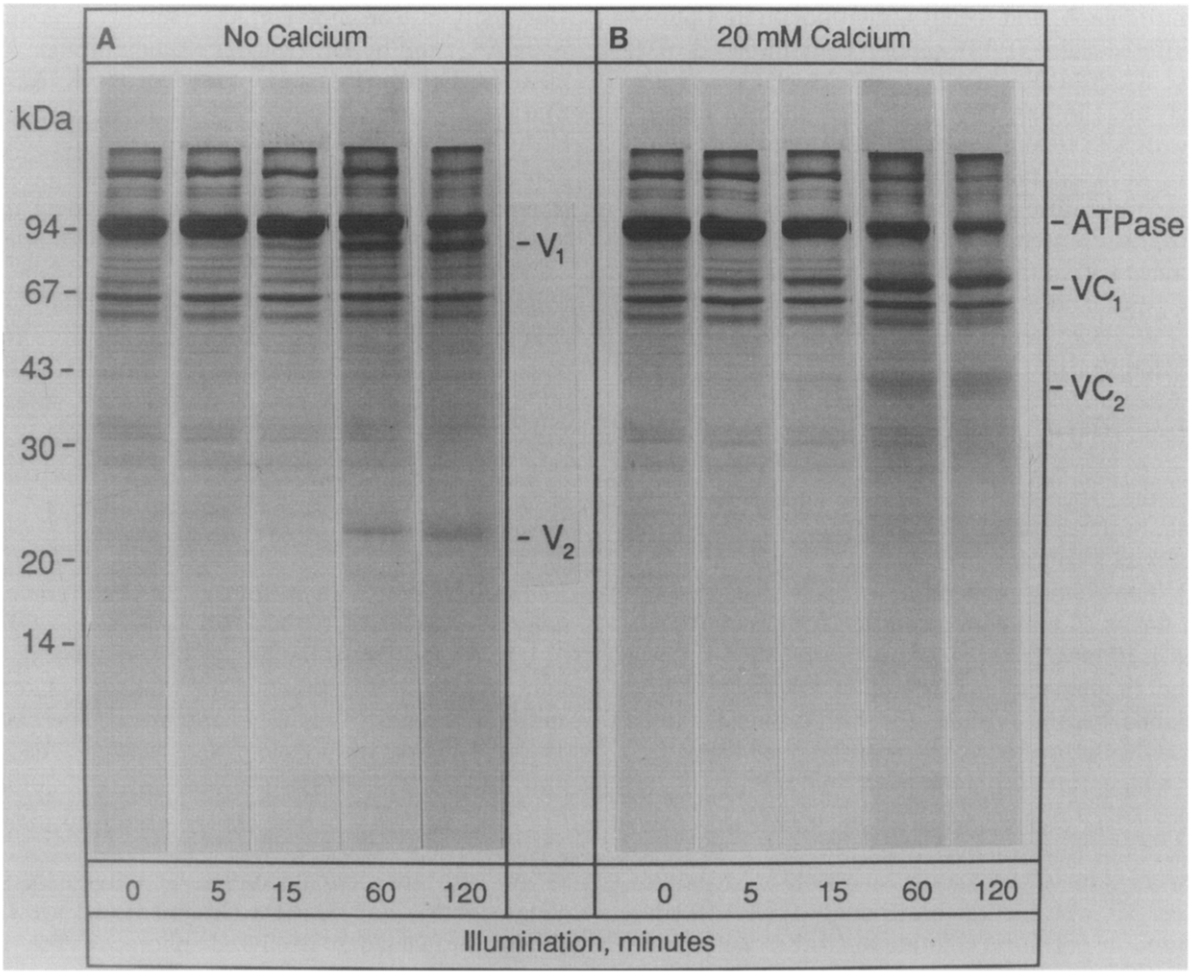

Fig. 1. Photocleavage of SR proteins induced by UV illumination in the presence of monovanadate. Sarcoplasmic reticulum vesicles (2 mg protein/ml) were suspended in a medium of 0.1 M KCl, 20 mM Hepes-K^+, 5 mM $MgCl_2$ (pH 7.0), 1 mM EGTA and 1 mM monovanadate, without (Fig. 1A), or with 20 mM $CaCl_2$ (Fig. 1B), and illuminated by ultraviolet light from 10 cm distance at 2° C for times ranging from 0 to 120 min. Aliquots containing 72 μg protein were taken at the indicated times for SDS-polyacrylamide gel electrophoresis. The dark band at ≅109 kDa is the Ca^{2+}-ATPase. The principal cleavage fragments are V_1 (87 kDa) and V_2 (22 kDa) in the absence of calcium (A), and 71 kDa (VC_1), 38 kDa (VC_2) in the presence of 20 mM Ca^{2+} (B).

tein that stains blue with Stains-All [62], while both the Ca^{2+}-ATPase and the products of the photocleavage stained red. Furthermore, quantitative densitometry of the bands of Ca^{2+}-ATPase and of the cleavage fragments stained with Coomassie blue indicates that the decrease in the amount of Ca^{2+}-ATPase during illumination was accompanied by a proportional increase in the amount of the cleavage products.

Analysis of the pH dependence of the monovanadate-catalyzed photocleavage at pH values ranging from 5 to 9 indicates a broad pH optimum between 7 and 8 in the absence of calcium and between 7 and 9 in the presence of 20 mM Ca^{2+} (not shown).

The effective vanadate concentration for the monovanadate-induced photocleavage was 1 mM in the absence of Ca^{2+}, and 0.1 mM in the presence of 20 mM Ca^{2+} (not shown). Decavanadate was ineffective in catalyzing photocleavage in the absence of Ca^{2+}, perhaps due to the absorption of ultraviolet light, but promoted the reaction in the presence of Ca^{2+}, producing fragments of the same size, at similar rate and at similar concentration as monovanadate.

The dependence of vanadate-induced photocleavage on Ca^{2+} concentration

The accessibility of the cleavage sites and the size of the cleavage products depends on the Ca^{2+} concentration of the medium (Fig. 2). When the free [Ca^{2+}] was lowered below 10^{-8} M by chelation with 1–10 mM EGTA, little or no cleavage of the Ca^{2+}-ATPase could be observed with 1 mM decavanadate, while monovanadate produced the characteristic V_1 and V_2 fragments of 87 kDa and 22 kDa, respectively. In the presence of 0.1–20 mM Ca^{2+} both monovanadate and decavanadate yielded the same cleavage products of 71 kDa (VC_1) and 38 kDa (VC_2), respectively; the rate of

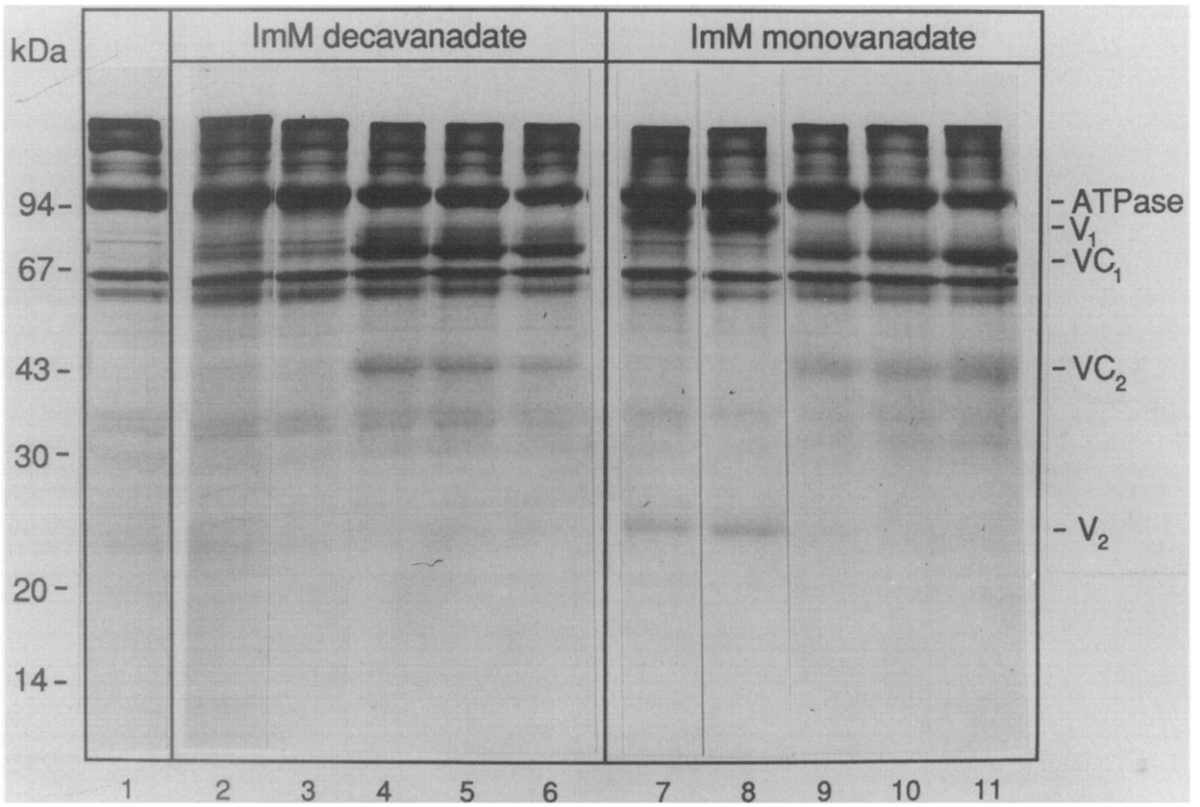

Fig. 2. Photocleavage of SR proteins at various Ca^{2+} concentrations. Sarcoplasmic reticulum vesicles (2 mg protein/ml) were suspended in a medium of 0.1 M KCl, 20 mM Hepes (pH 7.0), 5 mM $MgCl_2$, supplemented either with 1 mM decavanadate (lanes 2–6), or 1 mM monovanadate (lanes 7–11) and EGTA or $CaCl_2$ at concentrations given below. The samples were illuminated at 5 cm distance from an ultraviolet lamp at 2° C for 90 min. Aliquots of 70 μg protein were applied for SDS gel electrophoresis. The concentrations of EGTA and Ca^{2+} were as follows: lane 1, 20 mM Ca, no vanadate; lanes 2 and 7, 10 mM EGTA; lanes 3 and 8, 1 mM EGTA; lanes 4 and 9, 0.1 mM $CaCl_2$; lanes 5 and 10, 1 mM $CaCl_2$; lanes 6 and 11, 20 mM $CaCl_2$.

photocleavage in the presence of monovanadate increased with increasing Ca^{2+} concentrations from 0.1 to 20 mM, while in the presence of decavanadate the rate of cleavage remained largely unchanged in the range of 0.1–20 mM Ca^{2+}.

The requirement for millimolar Ca^{2+} concentration for the VC type cleavage to occur (Fig. 2) may arise from stabilization of the enzyme by vanadate in a conformation (E_2V) that has relatively low affinity for Ca^{2+}.

There is no indication that V and VC type cleavages of the Ca^{2+}-ATPase would occur concurrently under any of the conditions that we tested. Therefore the enzyme is apparently locked either in the conformation that permits the V type, or in the conformation that permits the VC type cleavage. The transition between the two major conformations is likely to be highly cooperative, so that equilibrium mixtures containing both conformations of the Ca^{2+}-ATPase would exist only in a narrow range of Ca^{2+} concentrations, that could be easily overlooked. Alternatively, if an intermediate conformation of Ca^{2+}-ATPase exists at μmolar Ca^{2+} concentrations, it may be relatively insensitive to photolysis.

The dependence of vanadate-induced photocleavage on the wavelength of the exciting light

The cleavage patterns of Ca^{2+}-ATPase were investigated with mono- or decavanadate as catalysts, in the presence of 20 mM Ca^{2+} or 1 mM EGTA, using lights of different wavelengths for excitation, isolated from the spectrum of the ultraviolet lamp by appropriate filters. The series of Schott filters: WG 280, WG 305, WG 335, GG 395 and GG 435 had 50% transmittance at the wavelengths indicated by the code numbers. In addition, Corning CS-056, CS-053 and CS-052 filters were also used with 50% transmittance near 280, 310 and 360 nm, respectively. The photocleavage in the presence of Ca^{2+} and monovanadate occurred at a broad range of wavelengths between 253 and 305 nm, but decreased significantly above 335 nm; the decrease with increasing wavelength was more pronounced in the absence of Ca^{2+}, where little cleavage occurred above 280 nm. The decavanadate-catalyzed photocleavage was

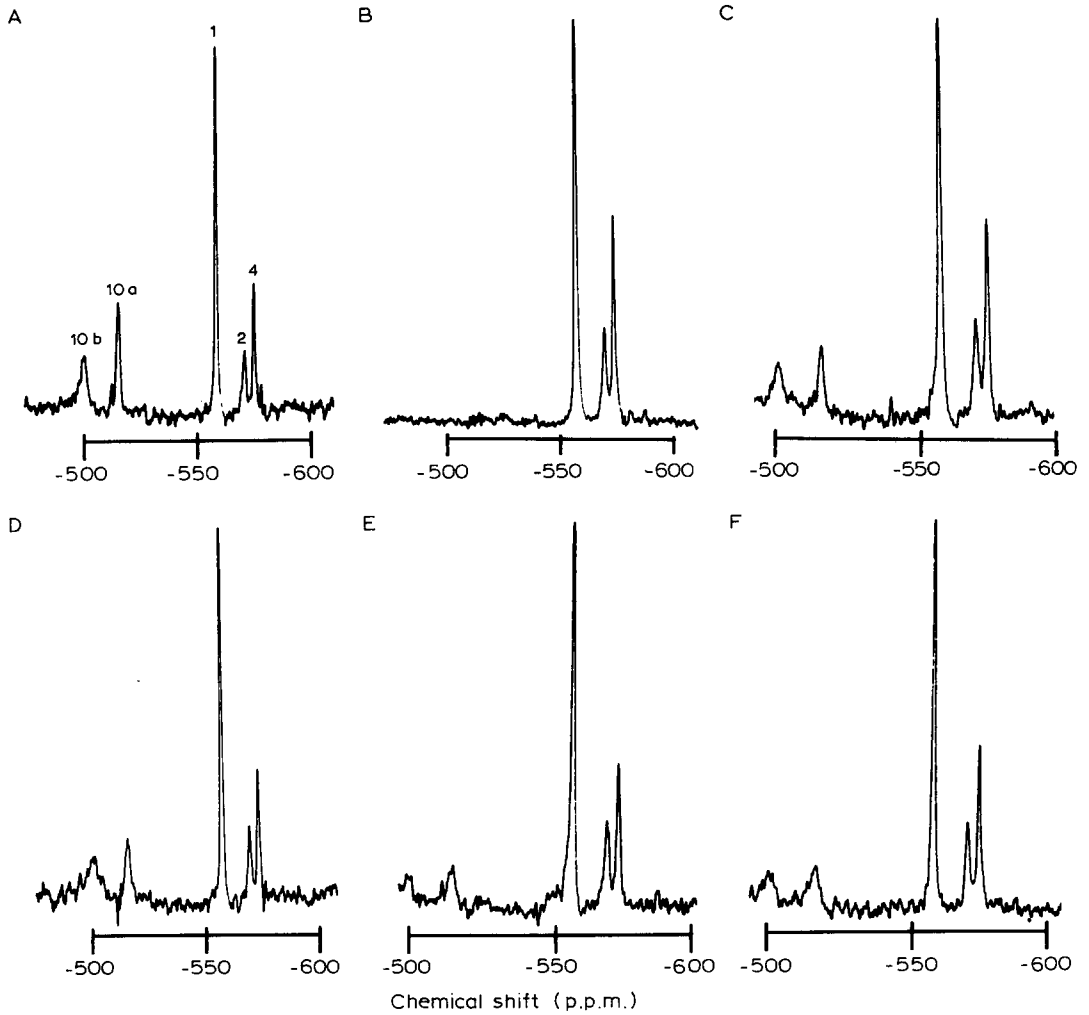

Fig. 3. ^{51}V-NMR spectra of vanadate species after ultraviolet illumination. The medium contained 0.1 M KCl, 20 mM Hepes (pH 7.0), 5 mM $MgCl_2$, 1 mM EGTA and a mixture of monovanadate and decavanadate (0.5 mM each) without added Ca^{2+} (panels A, B, D, E), or with 2 mM Ca added (panels C, F). Samples D, E, F also contained sarcoplasmic reticulum vesicles (2 mg protein/ml). Spectra A and D were taken before illumination; spectra B, C, E and F were taken after illumination for 90 minutes at 2°C from a distance of 5 cm. In panel A the bands corresponding to the various vanadate species are identified as follows: 1, monovanadate; 2 and 4, oligovanadates; 10a and 10b, decavanadate.

relatively weak, even at 280 nm (not shown). The wavelength dependence of photocleavage did not correspond to the absorption spectrum of aromatic amino acids or to that of monovanadate [63].

^{51}V-NMR analysis of vanadium (V) oligoanions

To determine whether ultraviolet irradiation changes the oxidation state of vanadate, the NMR spectra of vanadate solutions were analyzed in the presence and absence of sarcoplasmic reticulum under the conditions used for photocleavage of Ca^{2+}-ATPase.

Vanadium (V) in aqueous solution forms a complex equilibrium mixture of mono-, di-, tri-, tetra-, hexa- and decavanadates [44,45,53], that can be resolved by ^{51}V-NMR spectroscopy. As shown in Fig. 3 (A, B), ultraviolet illumination of a vanadate solution containing the various vanadate species, in the presence of 1 mM EGTA, selectively decreased the amplitude of the decavanadate components of the spectrum. This change was accompanied by a conversion of the characteristic yellow color the decavanadate solution first to a bluish-green and later to a gray color. Ca^{2+} ions (Fig. 3C) and sarcoplasmic reticulum vesicles (Fig. 3D, E, F) moderated the change in the decavanadate concentration induced by the ultraviolet light. The distribution of mono- and oligovanadates in the solutions was not affected significantly by irradiation in the presence of sarcoplasmic reticulum. Although these observations do not exclude changes in the oxidation state or mono-oligomer equilibrium of vanadate during illumination of sarcoplasmic reticulum, there is no indication that such changes would contribute to the observed photocleavage of Ca^{2+}-ATPase.

Reduced glutathione (25 mM) prevented the photo-

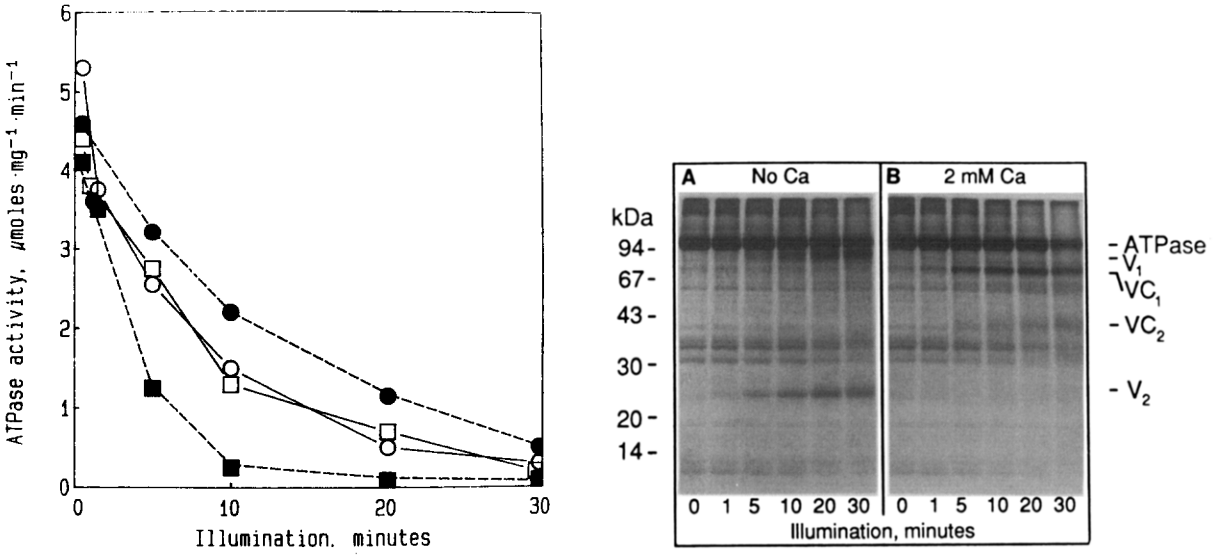

Fig. 4. Changes in the Ca^{2+}-ATPase activity of purified ATPase preparations during ultraviolet illumination. Purified Ca^{2+}-ATPase vesicles (2 mg protein per ml) prepared according to Meissner et al. [51] were illuminated by ultraviolet light from 2 cm distance at 2° C in a medium containing 0.1 M KCl, 20 mM Hepes (pH 7.0), 5 mM $MgCl_2$ and 1 mM EGTA, with or without 1 mM monovanadate, in the presence or absence of 2 mM $CaCl_2$. After 1, 5, 10, 20 and 30 min illumination, aliquots were taken to measure Ca^{2+}-ATPase activity and to check photocleavage by SDS-polyacrylamide gel electrophoresis. ○———○, Ca^{2+}-ATPase activity of samples illuminated in the absence of Ca^{2+} and vanadate; ●– – –●, samples illuminated with 2 mM $CaCl_2$, but no vanadate; □———□, samples illuminated without added Ca^{2+}, but with 1 mM vanadate; ■– – –■, samples illuminated with 2 mM $CaCl_2$ and 1 mM vanadate. The right-hand panel shows the electrophoretic patterns of the vanadate-containing samples without Ca (A) and with 2 mM Ca (B). In the absence of vanadate no detectable cleavage occurred whether or not Ca^{2+} was present.

cleavage of Ca^{2+}-ATPase by vanadate and under these conditions the expected vanadium(V) to vanadium(IV) conversion was, in fact, observed.

Do oxygen radicals play a role in the vanadate-catalyzed photocleavage?

The color changes of calcium-free decavanadate solutions during ultraviolet illumination, from yellow through greenish-blue, to grey, and finally, after several hours at room temperature, to colorless suggest the formation of reduced vanadium(IV) species. These may be partially reoxidized by dioxygen and could form various vanadyl-oxy compounds [64–66]. Some of these oxy radicals may be responsible for the vanadate-sensitized photocleavage, although superoxide dismutase, catalase, and horseradish peroxidase (20 to 100 U/ml), alone or in combination, had no effect on the vanadate-catalyzed photocleavage of Ca^{2+}-ATPase, with or without Ca^{2+}. Also without effect were bilirubin, α-tocopherol, or β-carotene (0.01–0.1 mM), carnosine and urate (0.1–1 mM).

Free radical scavengers and antioxidant enzyme mixtures did not reduce significantly the aggregation of sarcoplasmic reticulum proteins that accompanied irradiation. Neither did they protect against the loss of ATPase activity during illumination either with or without vanadate.

Effect of ultraviolet illumination on the ATPase and p-nitrophenylphosphatase activities of sarcoplasmic reticulum

During illumination by unfiltered ultraviolet light there was a steady loss of Ca^{2+}-stimulated ATPase and *p*-nitrophenylphosphatase activity (Fig. 4, Table I),

TABLE I

p-Nitrophenylphosphatase activity of Ca^{2+}-ATPase after 20 minutes ultraviolet illumination

Purified Ca^{2+}-ATPase was illuminated for 20 min at 2° C, as described in Fig. 4. Aliquots containing 100 μg protein were taken before and after illumination for measurement of the ATPase and *p*-nitrophenyl phosphatase activities, as described in Methods.

Mono-vanadate (mM)	$CaCl_2$ (mM)	ATPase ($\mu mol \cdot mg^{-1} \cdot min^{-1}$)		Inhibition of ATPase (%)	*p*-Nitrophenyl phosphatase ($nmol \cdot mg^{-1} \cdot min^{-1}$)		Inhibition of *p*-nitrophenyl-phosphatase (%)
		control	illuminated		control	illuminated	
0	0	5.8	2.09	64	32.0	18.6	42
0	2	5.8	1.98	66	32.0	18.6	42
1	0	5.8	1.68	71	21.8	11.3	48
1	2	5.8	0.33	94	25.5	1.1	96

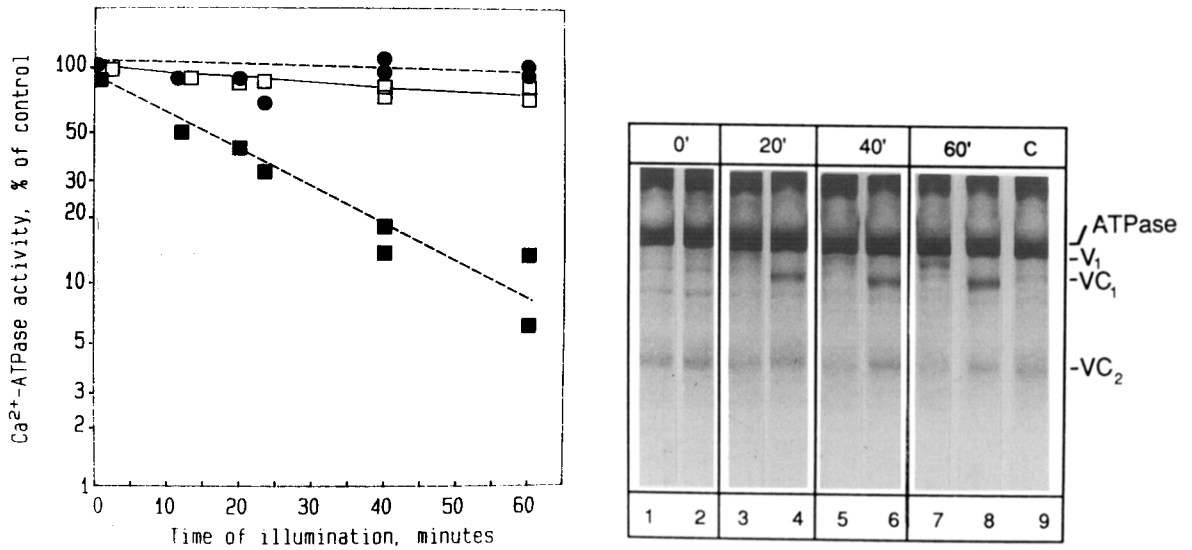

Fig. 5. The ATPase activity of sarcoplasmic reticulum after illumination with light filtered by CS-052 filter. Purified Ca^{2+}-ATPase vesicles (2 mg protein/ml) were illuminated by ultraviolet light passed through a CS-052 filter (Corning) for 0, 12, 20, 25, 40 and 60 min under conditions described in Fig. 4. After illumination, aliquots were taken for measurement of ATPase activity and to check photocleavage by gel electrophoresis. Symbols: ●– – –●, no vanadate, 2 mM $CaCl_2$; □———□, 1 mM vanadate, no Ca^{2+}; ■– – –■, 1 mM vanadate, 2 mM $CaCl_2$. The ATPase activity of the control samples taken at 0 time without illumination ranged between 4.55 and 6.45 $\mu mol \cdot mg^{-1} \cdot min^{-1}$. The data are collected from two identical experiments, carried out on different purified ATPase preparations. The values are expressed as percent of control values on a logarithmic scale. The right-hand panel, shows the cleavage pattern of Ca^{2+}-ATPase from one of these two experiments after 0 (lanes 1, 2), 20 (lanes 3, 4), 40 (lanes 5, 6) and 60 (lanes 7, 8) min of illumination in the presence of 1 mM vanadate and either no Ca^{2+} (samples 1, 3, 5, 7) or 2 mM Ca^{2+} (samples 2, 4, 6, 8). Lane 9 contains control sample (C) illuminated for 90 min in the presence of 2 mM Ca^{2+} but in the absence of vanadate.

without clear relationship to the cleavage of the polypeptide chain. Calcium (2 mM) slowed the light-induced loss of ATPase activity in the absence of vanadate, but accelerated the inhibition of ATP hydrolysis when 1 mM monovanadate was present (Fig. 4). Both ATPase and *p*-nitrophenylphosphatase activities were nearly completely lost after 20 minutes of irradiation in the presence of 1 mM vanadate and 2 mM $CaCl_2$

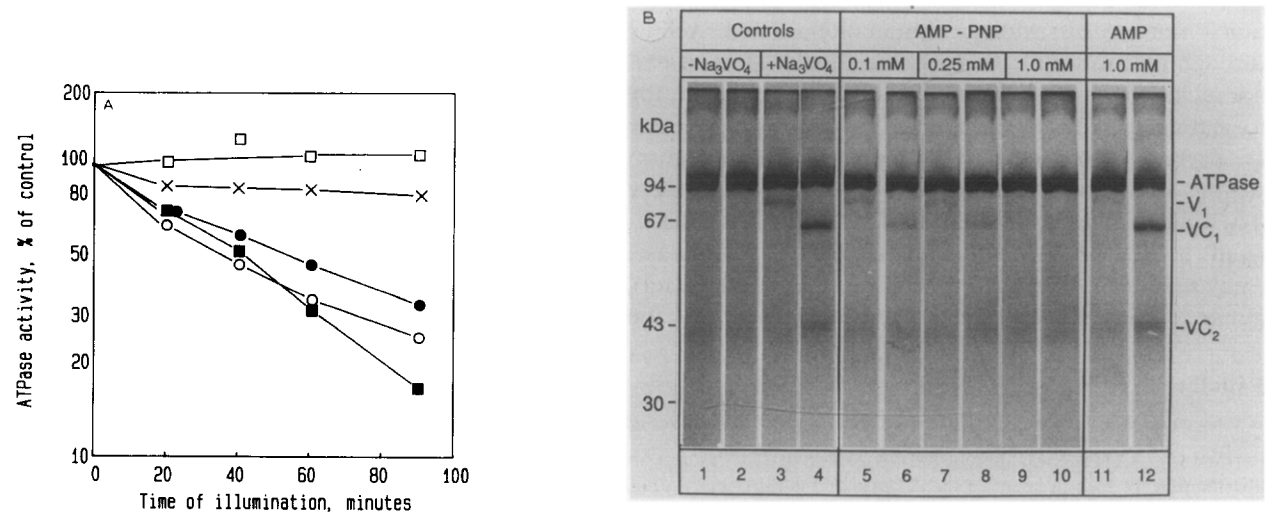

Fig. 6. Effect of AMP-PNP, AMP and ADP on the photoinactivation and photocleavage of Ca^{2+}-ATPase by monovanadate in the presence of 2 mM $CaCl_2$. The purified Ca^{2+}-ATPase (2 mg protein/ml) was illuminated at 2°C by unfiltered or CS-052 filtered light, in a medium of 0.1 M KCl, 10 mM imidazole (pH 7.0), 5 mM $MgCl_2$, 1 mM EGTA, 2 mM $CaCl_2$ with or without 1 mM monovanadate, in the absence of nucleoside phosphates or in the presence of 1 mM AMP, 1 mM AMP-PNP, or 1 mM ADP, for times ranging between 0 and 90 min. Aliquots were taken at intervals for assay of ATPase activity (A) and for SDS-polyacrylamide gel electrophoresis (B). (Panel A) ATPase activity measurements were made using light filtered with CS-052 filter. Symbols: □, no vanadate; ■, with 1 mM monovanadate but no nucleoside phosphates; ×, 1 mM vanadate and 0.25 mM AMP-PNP; ○, 1 mM vanadate and 0.25 mM AMP; ●, 1 mM vanadate and 0.25 mM ADP. (Panel B) The photocleavage was detected by SDS-polyacrylamide gel electrophoresis after illumination with unfiltered light. The samples in odd-numbered lanes were illuminated without, and those in even numbered lanes with 2 mM $CaCl_2$. Samples: 1 and 2, no vanadate, 3–12, 1 mM monovanadate; 3 and 4, no nucleotide; 5 and 6, 0.1 mM AMP-PNP; 7 and 8, 0.25 mM AMP-PNP; 9 and 10, 1.0 mM AMP-PNP, 11 and 12, 1 mM AMP.

(Table I). The faster loss of ATPase activity during illumination in the presence of calcium is consistent with simultaneous binding of vanadate and calcium to the Ca^{2+}-ATPase [67–69].

The observations shown in Fig. 4 indicate that at least two separate processes contribute to the inhibition of ATPase activity during illumination by ultraviolet light, only one of which is vanadate-dependent. The vanadate-independent component of inactivation could be largely prevented using the Corning CS-052 filter to isolate the long wavelength components of the exciting light. The CS-052 filter has less than 10% transmittance at or below 350 nm, with 50% transmittance near 360 nm. Under these conditions there was no loss of ATPase activity during illumination in a Ca^{2+}-free system for up to 60 min either in the presence or absence of 1 mM vanadate, but illumination with 1 mM vanadate and 2 mM $CaCl_2$ produced a steady loss of ATPase activity with first-order kinetics (Fig. 5). The photoinactivation catalyzed by vanadate + Ca^{2+} (Fig. 5), was accompanied by the photocleavage of the Ca^{2+}-ATPase at the VC site, forming the large VC_1 fragment of 71 kDa and the smaller VC_2 fragment of 38 kDa (Fig. 5, right-hand panel). Only slight cleavage of Ca^{2+}-ATPase was observed during illumination with vanadate in the presence of EGTA, i.e., at a free Ca^{2+} concentration below 10^{-8} M, consistent with the retention of ATPase activity. The use of filtered light did not prevent the moderate aggregation of Ca^{2+}-ATPase during illumination that was observed with or without vanadate.

The effect of substrate analogues on the vanadate-catalyzed photocleavage and photoinhibition of ATPase activity

Vanadate is a substrate analogue of inorganic phosphate that is presumed to interact in or near the active site of the Ca^{2+}-ATPase. Therefore the effect of inorganic phosphate and various nucleoside phosphates upon the vanadate-catalyzed photocleavage and photoinactivation of the Ca^{2+}-ATPase was investigated.

AMP-PNP (0.25–1 mM) significantly reduced the rate of vanadate-catalyzed photocleavage in the presence of either Ca^{2+} or EGTA (Fig. 6B). The inhibition of photocleavage by AMP-PNP was accompanied by protection of ATPase activity (Fig. 6A).

The specific requirement for AMP-PNP for this protection, while AMP had no significant effect rules out the possibility that the protective effect is due to the absorption of light. This is unlikely in any case, since the protection was also observed in experiments using CS-052 filters that eliminated the spectral components that would be absorbed by AMP-PNP. The small but significant protection provided by ADP against photoinactivation (Fig. 6A) may be due either to a direct effect of ADP or to ATP formed in the system by traces of myokinase.

We attribute the protection by AMP-PNP and by ADP/ATP to competition between the nucleoside phosphates and vanadate for binding sites on the Ca^{2+}-ATPase. The lack of effect of AMP implies that the β- and γ-phosphate groups are essential for competition either because they have a common binding site with vanadate, or because their presence increases the affinity of the nucleoside phosphate for the enzyme, making it a more effective competitor with vanadate. These experiments increase the likelihood that the vanadate-catalyzed photocleavage occurs in the ATP binding domain.

Inorganic phosphate up to 20 mM concentration had no detectable influence on the photocleavage at pH 7.0 in the presence of 1 mM monovanadate and either 1 mM EGTA or 1 mM EGTA and 2 mM Ca^{2+} (not shown). This is probably attributable to the relatively low affinity of P_i for the enzyme relative to vanadate at pH 7.0. Since the ATPase activity was not affected significantly by illumination with CS-052 filtered light in the presence of 1 mM monovanadate and 1 mM EGTA (Fig. 5), the effect of inorganic phosphate on the vanadate-catalyzed photocleavage was not investigated further.

Vanadate-catalyzed photocleavage of the tryptic fragments of the Ca^{2+}-ATPase

Trypsin preferentially cleaves the Ca^{2+}-ATPase at the T_1 cleavage site, between Arg-505 and Ala-506, into the A and B fragments. In the presence of EGTA and vanadate further cleavage of the Ca^{2+}-ATPase at the T2 site is blocked [30,36] and a digest of relatively simple composition can be obtained (Figs. 7 and 8, lane 7). The B fragment can be selectively labeled with FITC on Lys-515 [15,27], permitting its identification on SDS-polyacrylamide gels by fluorescence (Figs. 7 and 8, lane 8). No difference was found in the photocleavage pattern of T_1 cleaved fragments, whether the FITC labeling of the sample was carried out before or after illumination (not shown).

The products of the monovanadate-catalyzed photocleavage of intact Ca^{2+}-ATPase in the absence of Ca^{2+} were fragments V_1 and V_2 (Fig. 7, lane 3); the V_1 fragment is strongly fluorescent (Fig. 7, lane 4), indicating that it contains Lys-515. In the presence of Ca^{2+} the monovanadate-catalyzed photocleavage of Ca^{2+}-ATPase at the VC site yields the strongly fluorescent VC_1 fragment, together with VC_2, that is nonfluorescent (Fig. 7, lanes 5, 6).

Use of the A and B tryptic fragments (Fig. 7, lanes 7 and 8) for photocleavage in the presence of monovanadate, permitted closer localization of the photocleavage sites. Photocleavage in the absence of Ca^{2+} (Fig. 7, lane 9) produced the V_1A subfragment of 35 kDa, together with the V_2 fragment of the same size (22 kDa) as was obtained after photocleavage of the intact ATPase.

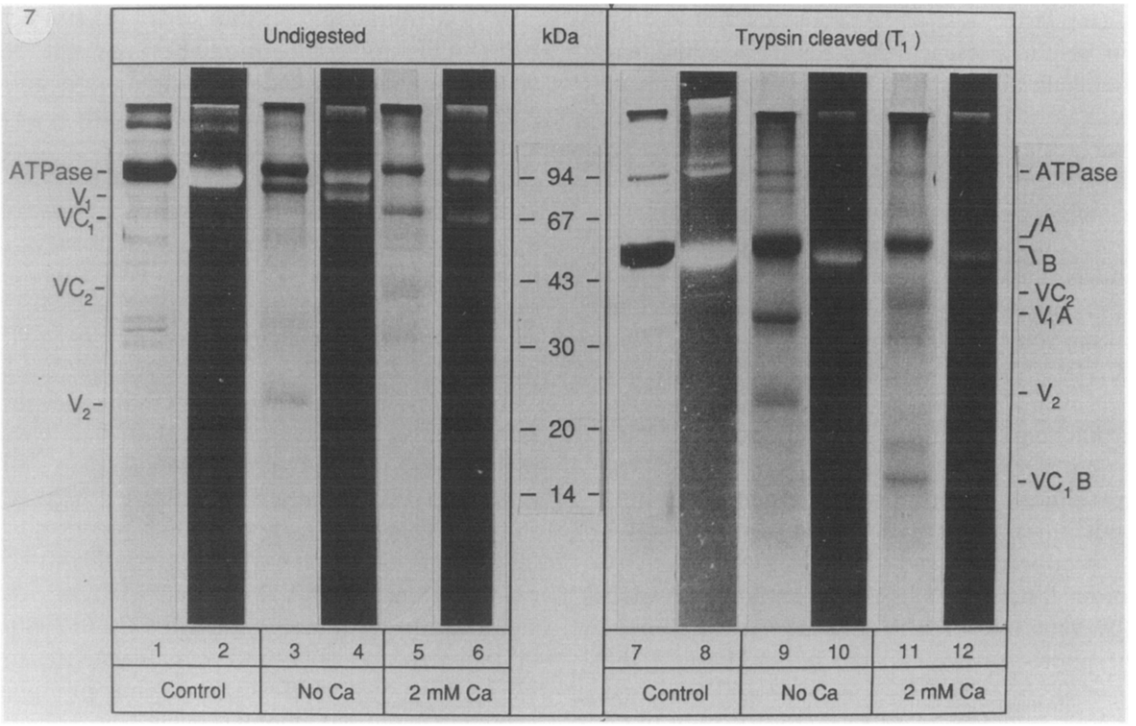

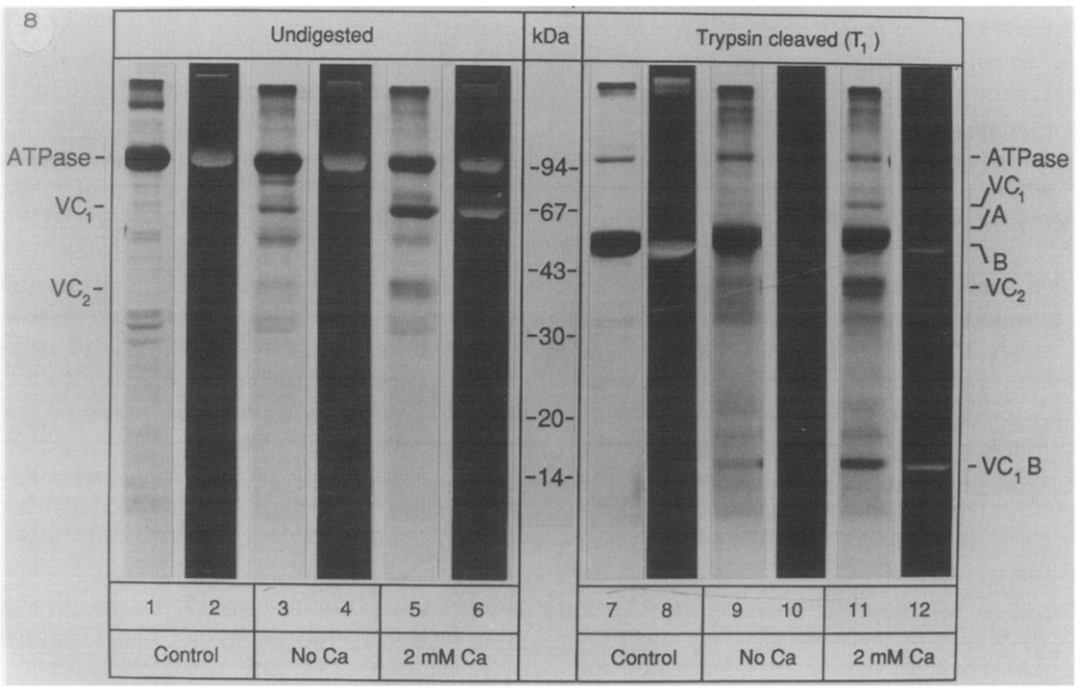

Fig. 7 and 8. Photocleavage of Ca^{2+}-ATPase and its tryptic fragments. Tryptic fragments of Ca^{2+}-ATPase prepared by trypsin digestion of purified ATPase preparations (2 mg/ml protein) were illuminated by ultraviolet light in a medium of 0.1 M KCl, 20 mM Hepes-K^+, pH 7, 5 mM $MgCl_2$, 1 mM EGTA, and either 1 mM monovanadate (Fig. 7, top), or 1 mM decavanadate (Fig. 8, bottom), in the presence or absence of 2 mM $CaCl_2$. After 90 min illumination at 2°C, from 5 cm distance, EGTA (2 mM) was added and the pH was adjusted with dilute NaOH to pH 8.1. The samples were reacted with FITC (7 nmol/mg protein) at 25°C for 30 min in the dark, as described earlier [31]. Aliquots of 100 μg protein were prepared for SDS polyacrylamide gel electrophoresis. The FITC-labeled fragments were visualized by fluorescence and photographed before staining the gels for protein. Lanes 1, 2, 7 and 8 are controls (no Ca^{2+} and vanadate added and not illuminated); lanes 3, 4, 9, 10 are samples illuminated in the presence of vanadate without added Ca^{2+}; lanes 5, 6, 11 and 12 are samples illuminated in the presence of vanadate and 2 mM Ca^{2+}. Lanes 1–6: undigested Ca^{2+}-ATPase; lanes 7–12: tryptic fragments of Ca^{2+}-ATPase. Odd-numbered lanes: samples stained with Coomassie blue; even-numbered lanes: fluorescence of FITC-labeled fragments.

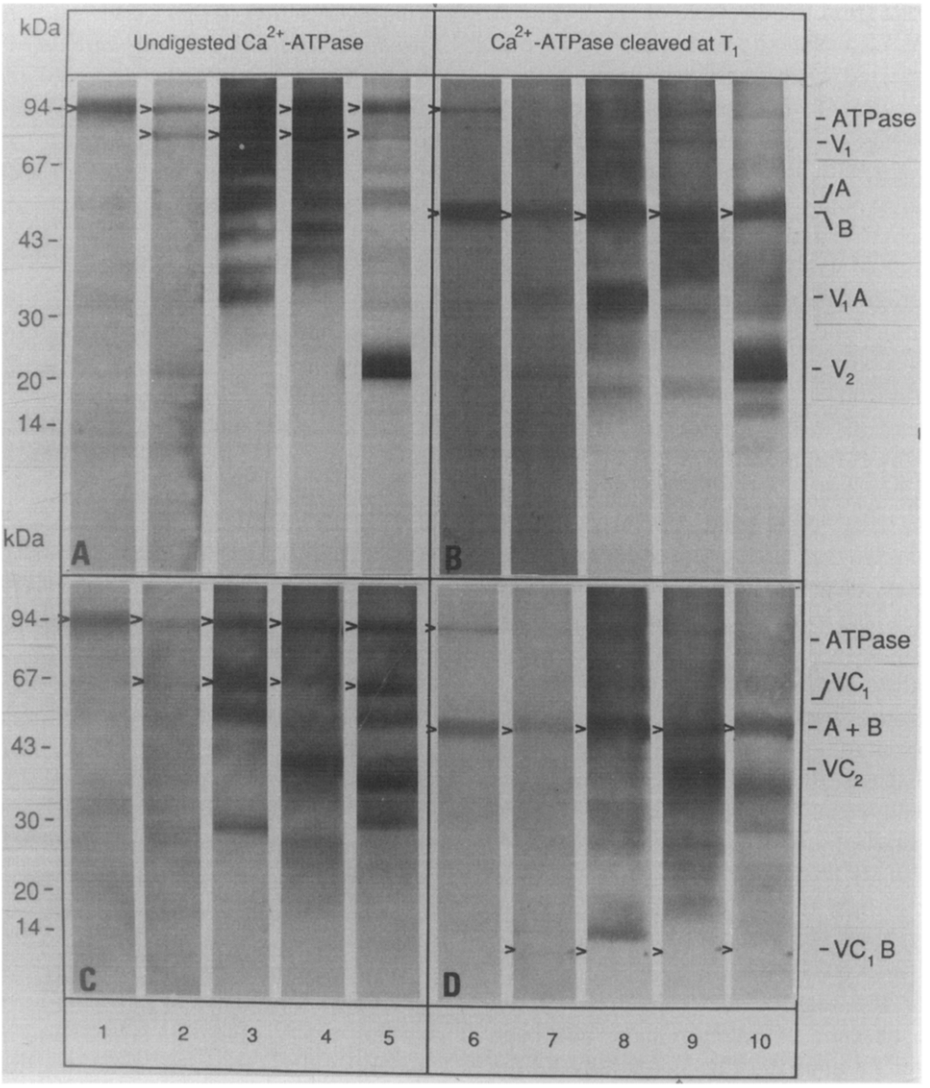

Fig. 9. Immunoreaction of the products of the vanadate-catalyzed photocleavage of Ca^{2+}-ATPase by monoclonal and polyclonal antibodies. (a) Undigested Ca^{2+}-ATPase (A, C). Purified Ca^{2+}-ATPase preparations (2 mg protein/ml) were suspended in a medium of 0.1 M KCl, 20 mM K^+-Hepes (pH 7.0), 5 mM $MgCl_2$, 1 mM EGTA and 1 mM monovanadate, without added Ca^{2+} (Fig. 9A), or with 2 mM Ca (Fig. 9C). After illumination with an ultraviolet lamp for 90 min at 2°C from a distance of 5 cm, the protein fragments were separated by SDS-polyacrylamide gel electrophoresis on 6–18% gradient gels, transferred to nitrocellulose sheets, and either stained with Amido black or reacted with anti-ATPase antibodies, as described under Methods. (b) Ca^{2+}-ATPase after limited proteolysis (B, D). Proteolysis with trypsin (50 μg/ml) was performed in a medium of 0.1 M KCl, 20 mM K^+-Hepes (pH 7.0), 5 mM $MgCl_2$, 1 mM EGTA, and 1.0 mM monovanadate, at a microsomal protein concentration of 2 mg/ml at 25°C for 15 min; the reaction was stopped with 200 μg/ml soybean trypsin inhibitor. Monovanadate (1 mM) was added to limit the cleavage of the Ca^{2+}-ATPase to the T_1 site, resulting in the formation of two major fragments, A and B [30,31,36]. The samples were washed with a solution of 0.1 M KCl, 20 mM K^+-Hepes (pH 7.0), 5 mM $MgCl_2$, 1 mM EGTA and 50 μg/ml trypsin inhibitor by centrifugation at 105000 × *g* for 45 min. The pellets were resuspended in the same solution without trypsin inhibitor and the samples were subjected to vanadate-catalyzed photocleavage without added Ca^{2+} (Fig. 9B) or with 2 mM Ca (Fig. 9D), as described above for the intact Ca^{2+}-ATPase. Aliquots of the photocleaved samples were reacted with fluorescein 5′-isothiocyanate, as described in Methods, to identify the fragments that contain the reactive Lys-515 as the marker of the B fragment. After transfer to nitrocellulose sheets the reaction with antibodies was performed as described under Methods. Each sample contained 30 μg of sarcoplasmic reticulum proteins. Anti-ATPase antibodies were diluted 1:1000 for reaction and the bound antibodies were detected using peroxidase conjugated anti-host IgG antibody. Arrows mark the location of bands that showed intense fluorescence due to FITC covalently bound to Lys-515. Lane 1, purified Ca^{2+}-ATPase (control; Amido black staining); lanes 2–5, purified Ca^{2+}-ATPase after ultraviolet irradiation; lane 2, Amido black-stained fragments; lane 3, immunostaining with anti-A_1 (7C6) antibody; lane 4, immunostaining with anti-B (A52) antibody; lane 5, immunostaining with anti-A_2 (EM-1) antibody; lane 6, purified Ca^{2+}-ATPase after tryptic cleavage at the T_1 site (Amido black staining); lanes 7–10, purified Ca^{2+}-ATPase after tryptic cleavage at the T_1 site and ultraviolet irradiation. Lane 7, Amido black staining of fragments; lane 8, immunostaining with anti-A_1 (7C6) antibody; lane 9, immunostaining with anti-B (A52) antibody; lane 10, immunostaining with anti-A_2 (EM-1) antibody.

These fragments arise from the cleavage of the tryptic A fragment at the V cleavage site near the T_2 tryptic cleavage site; as expected, both fragments were nonfluorescent. The fluorescent B fragment remained unaffected by photocleavage in the absence of calcium (Fig. 7, lane 10), consistent with the location of the V cleavage site in the A fragment.

Monovanadate-catalyzed photocleavage of the tryptic digest in the presence of Ca^{2+} produced a small, highly fluorescent VC_1B fragment of 14 kDa (Fig. 7, lanes 11 and 12) that contains the region of the B fragment between the T_1 cleavage site (Ala-506) and the VC cleavage site; in addition, a somewhat diffuse nonfluorescent VC_2 fragment of $\cong$ 38 kDa formed, that represents the region of the B fragment from the VC cleavage site to its C-terminus (Fig. 7, lane 11). Some other fragments were also observed in small amounts, indicating additional photocleavage sites exposed by calcium.

These observations clearly establish the location of the V type photocleavage in the A fragment near the T_2 tryptic cleavage site and of the VC type photocleavage in the N-terminal third of the B fragment.

There are significant differences in the photocleavage catalyzed by monovanadate (Fig. 7) and decavanadate (Fig. 8). In the absence of added Ca^{2+} decavanadate was much less effective than monovanadate in catalyzing the photocleavage of intact Ca^{2+}-ATPase (Fig. 8, lanes 3 and 4), or of its tryptic cleavage products (Fig. 8, lanes 9 and 10); in fact, the slight photocleavage that was observed may have occurred at the VC cleavage site.

The reasons for the relative ineffectiveness of decavanadate in the absence of calcium have not been investigated in detail; a contributing factor may be the strong absorption of light by the yellow decavanadate solution in the ultraviolet region of the spectrum, where the light energy optimum for photocleavage is located.

By contrast, decavanadate effectively catalyzed the photocleavage of Ca^{2+}-ATPase at the VC cleavage site in the presence of calcium, yielding the highly fluorescent VC_1 fragment of 71 kDa and the nonfluorescent VC_2 fragment of 38 kDa (Fig. 8, lanes 5 and 6), as observed with monovanadate (Fig. 7). Similarly, the decavanadate-catalyzed photocleavage of the tryptic digest in the presence of Ca^{2+} (Fig. 8, lanes 11 and 12) produced the fluorescent VC_1B and the nonfluorescent VC_2 fragments, like monovanadate, while the A fragment remained unaffected. The VC_2 (38 kDa) fragment produced by deca- or monovanadate was diffuse and occasionally appeared as a doublet (Fig. 8, lanes 5 and 11), raising the possibility that the VC cleavage may occur at two nearby sites, or that there was some heterogeneity in the Ca^{2+}-ATPase population due to the presence of slow and fast Ca^{2+}-ATPase isoenzymes.

Immunoreaction of the Ca^{2+}-ATPase and its cleavage products with anti-ATPase antibodies

To further define the origin of the V_1, V_2, VC_1, VC_2 fragments in the Ca^{2+}-ATPase molecule, three previously characterized anti-ATPase antibodies with defined antigenic sites on the Ca^{2+}-ATPase were used to identify the cleavage fragments, together with partial tryptic proteolysis and FITC labeling (Fig. 9). The antigenic determinant of the 7C6 monoclonal mouse antibody is on the A_1 tryptic fragment, while the A52 monoclonal mouse antibody reacts with an epitope between amino acid residues 659 and 668 in the B fragment of the Ca^{2+}-ATPase (Ref. 60; MacLennan, D.H., personal communication). The EM-1 polyclonal rabbit antibody preferentially reacts with the A_2 tryptic fragment. Fluorescein 5′-isothiocyanate was used to label Lys-515. Vanadate-sensitized photocleavage was performed both on the intact Ca^{2+}-ATPase and on Ca^{2+}-ATPase that was previously cleaved by trypsin at the T_1 cleavage site to form the A and B tryptic fragments.

The fragments produced by vanadate from the intact or trypsin-cleaved Ca^{2+}-ATPase were separated by electrophoresis on sodium dodecylsulfate polyacrylamide gradient gels (6–18%), followed by transfer of the proteins to nitrocellulose membranes for immunostaining (Fig. 9). Lanes 1 and 6 show the Amido black stained protein components of the samples before illumination, and lanes 2, 7 after ultraviolet illumination. Bands which contain fluorescent labels were marked by arrowheads.

After illumination in the absence of calcium the V_1 (87 kDa) fragment contains the antigenic determinants of the anti-A_1 (Fig. 9A, lane 3) and anti-B (Fig. 9A, lane 4) antibodies, together with the fluorescein 5′-isothiocyanate binding site. The anti-A_2 antibody reacts with the V_2 (22 kDa) fragment (Fig. 9A, lane 5). When the Ca^{2+}-ATPase was previously cleaved by trypsin at the T_1 site the anti-A_1 antibody reacts with the 35 kDa V_1A fragment (Fig. 9B, lane 8). The anti-B antibody stained the same B fragment as in the trypsin digested but not illuminated control sample (Fig. 9B, lane 9), while the anti-A_2 antibody binds to the same V_2 fragment (Fig. 9B, lane 10) as in the undigested Ca^{2+}-ATPase. These data confirm that the vanadate-catalyzed V type cleavage in the absence of calcium occurs in the A fragment close to the T_2 tryptic cleavage site.

After illumination of intact ATPase in the presence of calcium, two major fragments, VC_1 and VC_2, were formed. The VC_1 (71 kDa) fragment (Fig. 9C, lanes 2–5) contains the fluorescein 5′-isothiocyanate binding site and the antigenic determinants of the anti-A_1 and anti-A_2 antibodies (Fig. 9C, lanes 3–5). The anti-B antibody binds to the VC_2 (38 kDa) fragment of the Ca^{2+}-ATPase (Fig. 9C, lane 4). When Ca^{2+}-ATPase

previously cleaved with trypsin at the T_1 site into the A and B fragments was used, in addition to the uncleaved A fragment, a small 14 kDa VC_1B fragment formed that contained the FITC label bound to lysine 515 (Fig. 9D, lanes 7–10). The anti-A_1 and anti-A_2 antibodies both labeled the 57 kDa A fragment (Fig. 9D, lanes 8, 10), while the anti-B antibody reacted with the 38 kDa VC_2 fragment, indicating the presence of amino acids 659 through 668. The explanation of this pattern is that the vanadate-catalyzed VC type cleavage in the presence of calcium occurs between the FITC binding site (Lys-515) and the antigenic determinants of the A52 (anti-B) monoclonal antibody located at residues 659 through 668.

Discussion

Depending on the free calcium concentration of the medium, the vanadate-catalyzed photolysis of the Ca^{2+}-ATPase occurred at two distinct sites. At a free $[Ca^{2+}]$ of 10 nM or less, the apparent molecular mass of the primary cleavage prducts was $\cong$ 87 and $\cong$ 22 kDa. The 87 kDa V_1 fragment contained the FITC binding site and reacted with the 7C6 and A52 antibodies directed against the A_1 and B tryptic fragments of the Ca^{2+}-ATPase, while the 22 kDa fragment (V_2) reacted with the EM-1 antibody directed against the A_2 tryptic fragment. Based on these observations, we suggest that the vanadate-catalyzed photocleavage in the absence of

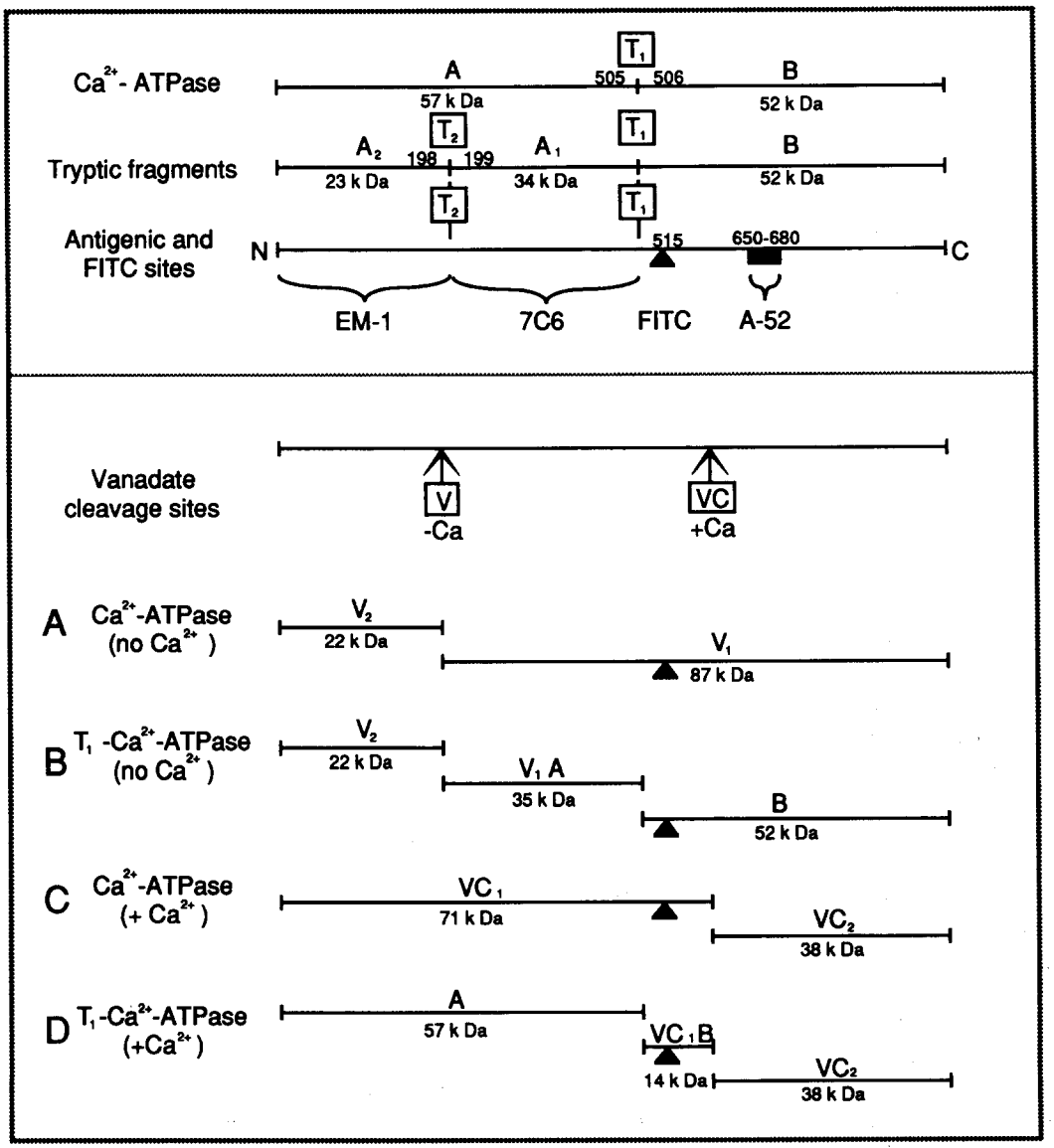

Fig. 10. The topography of cleavage sites in the Ca^{2+}-ATPase. A schematic illustration is provided for the distribution of tryptic and photolytic cleavage sites in the Ca^{2+}-ATPase, together with the designation, approximate size, and antibody specificity of the cleavage fragments. For details, see text. Sections A, B, C and D correspond to the experiments described in Fig. 9 A, B, C and D, respectively. T_1-Ca^{2+}-ATPase, Ca^{2+}-ATPase cleaved by trypsin at the T_1 site.

Ca^{2+} occurs at the V site near the T_2 cleavage site of the Ca^{2+}-ATPase (Arg-198-Ala-199), releasing the N-terminal 22 kDa fragment (V_2) that is similar in size and immunoreactivity to the A_2 fragment obtained by tryptic cleavage (Fig. 10). The large 87 kDa V_1 fragment is assumed to contain much of the A_1 + B regions of the molecule, extending to the C terminus.

Vanadata binds to the Ca^{2+}-ATPase with high affinity, inhibiting the Ca^{2+}-stimulated hydrolysis of ATP [27,70–73]. The inhibition is usually attributed to the formation of a stable E_2-V enzyme intermediate that cannot be phosphorylated by ATP. It is reasonable to assume that vanadate, as an analogue of inorganic phosphate, interacts with the Ca^{2+}-ATPase near the active site Asp-351, where during the normal course of the reaction the enzyme becomes covalently phosphorylated by ATP.

In the absence of calcium, vanadate blocks completely the tryptic cleavage of Ca^{2+}-ATPase at the T_2 site [30,31,36]. Considering the proposed folding patterns of the Ca^{2+}-ATPase, the T_2 cleavage site in the native enzyme may be near the phosphorylation site, where vanadate is likely to be bound. Therefore the proximity of vanadate to the T_2 cleavage site may explain both the vanadate-catalyzed photocleavage and the vanadate-induced inhibition of the tryptic cleavage of the enzyme in this region of the molecule [36].

Based on enzyme-linked immunoassay, the affinity of the Ca^{2+}-ATPase for the A52 monoclonal antibody directed against residues 659–668 was not influenced by the vanadate-catalyzed photocleavage, either in the presence or absence of Ca^{2+}. Similarly, there was no change in the affinity for A52 in T_1-cleaved Ca^{2+}-ATPase, either before or after ultraviolet illumination in the presence of vanadate.

The affinity of vanadate for tyrosine is $\cong 10^6$-fold greater compared with inorganic phosphate [46]. Photochemical modification of aromatic amino acids near the ATP binding site was invoked to explain the vanadate-catalyzed photocleavage of myosin [40,41,47], and a similar process may be involved in the sarcoplasmic reticulum Ca^{2+}-ATPase. Among the aromatic amino acids located in the general region of the molecule near the T_2 site are tyrosine 122, 130, 294, 295, tryptophan 107, 272, 288 and phenylalanine 209, 256, 279, 296. The cluster of tyrosine 294, 295 and phenylalanine 296 would be an interesting potential target.

In the presence of 2–20 mM Ca, the vanadate-catalyzed photocleavage of Ca^{2+}-ATPase yields two fragments of 71 kDa (VC_1) and 38 kDa (VC_2), respectively. The 71 kDa N-terminal fragment contained FITC fluorescence, indicating the presence of Lys-515, and was labeled by antibodies 7C6 and EM-1 directed against the A_1 and A_2 regions of the Ca^{2+}-ATPase, respectively (Fig. 10). Therefore the site of the vanadate-catalyzed photocleavage of Ca^{2+}-ATPase in the presence of 2–20 mM Ca (VC) is between Lys-515 and the C terminus of the Ca^{2+}-ATPase, in the region of the molecule that corresponds to the B tryptic fragment. Consistent with this interpretation, the A52 antibody with epitopes on amino acids 659–668 reacted only with the 38 kDa (VC_2) fragment but did not react with the 71 kDa (VC_1) fragment that included the FITC binding site (Lys-515). Vanadate-catalyzed photocleavage of the tryptic B fragment indeed released a 14 kDa polypeptide (VC1B) that contained the FITC binding site, indicating that it originated from the amino terminal end of the B fragment. The A tryptic fragment was not affected by irradiation in the presence of calcium and vanadate, indicating that under these conditions the V cleavage site is inactive.

The vanadate-sensitive cleavage site of the Ca^{2+}-ATPase in the absence of Ca^{2+} (V) is close to the T_2 tryptic cleavage site, while the cleavage site in the presence of Ca^{2+} (VC) is clearly distinct from the T_1 site attacked by trypsin. The high specificity of the cleavage indicated by the homogeneity of the cleavage products suggests that the two vanadate-sensitive regions in the molecule are alternately exposed, depending on the absence or presence of calcium in the medium. Either there are two distinct vanadate binding sites involved in the V and VC type cleavages, or vanadate bound at a single site may be brought by conformational changes of the enzyme into reaction with either the V cleavage site in the absence of calcium, or with the VC cleavage site in the presence of calcium. The identification of the amino acids modified during photocleavage and their localization in the sequence of Ca^{2+}-ATPase is in progress.

Acknowledgements

We express our thanks to Dr. Davis H. MacLennan and Dr. Douglas M. Fambrough for providing us with several anti-Ca^{2+}-ATPase antibodies that were used in these studies. This study was supported by research grants from the NIH (AR 26545), NSF (PCM 84-03679 and Int. 86-17848) and by the Muscular Dystrophy Association.

References

1 Migala, A., Agostini, B. and Hasselbach, W. (1973) Z. Naturforsch. Teil C 28, 178–182.
2 Stewart, P.S. and MacLennan, D.H. (1974) J. Biol. Chem. 249, 985–993.
3 Thorley-Lawson, D.A. and Green, N.M. (1973) Eur. J. Biochem. 40, 403–413.
4 Thorley-Lawson, D.A. and Green, N.M. (1975) Eur. J. Biochem. 59, 193–200.
5 Thorley-Lawson, D.A. and Green, N.M. (1977) Biochem. J. 167, 739–748.
6 Allen, G. and Green, N.M. (1978) Biochem. J. 173, 393–402.
7 Allen, G. (1980) Biochem. J. 187, 545–563.

8 Lüdi, H. and Hasselbach, W. (1984) FEBS Lett. 167, 33–36.
9 Allen, G. (1980) Biochem. J. 187, 565–575.
10 Allen, G., Bottomley, R.C. and Trinnaman, B.J. (1980) Biochem. J. 187, 577–589.
11 Tong, S.W. (1980) Arch. Biochem. Biophys. 203, 780–791.
12 Allen, G., Trinnaman, B.J. and Green, N.M. (1980) Biochem. J. 187, 591–616.
13 Green, N.M. and Toms, E.J. (1985) Biochem. J. 231, 425–429.
14 MacLennan, D.H., Brandl, C.J., Korczak, B. and Green, N.M. (1985) Nature (London) 316, 696–700.
15 Brandl, C.J., Green, N.M., Korczak, B. and MacLennan, D.H. (1986) Cell 44, 597–607.
16 Brandl, C.J., DeLeon, S., Martin, D.R. and MacLennan, D.H. (1987) J. Biol. Chem. 262, 3768–3774.
17 Korczak, B., Zarain-Herzberg, A., Brandl, C.J., Ingles, C.J., Green, N.M. and MacLennan, D.H. (1988) J. Biol. Chem. 263, 4813–4819.
18 Lytton, J. and MacLennan, D.H. (1988) J. Biol. Chem. 263, 15024–15031.
19 Lytton, J., Zarain-Herzberg, A., Periasamy, M. and MacLennan, D.H. (1989) J. Biol. Chem. 264, 7059–7065.
20 Green, N.M., Taylor, W.R., Brandl, C., Korczak, B. and MacLennan, D.H. (1986) in Calcium and the Cell, CIBA Foundation Symp. 122, pp. 93–107, John Wiley & Sons, Chichester.
21 Green, N.M., Taylor, W.R. and MacLennan, D.H. (1988) in The Ion Pumps: Structure, Function, and Regulation (Stein, W.D., ed.), pp. 15–24, Alan R. Liss, New York.
22 Taylor, W.R. and Green, N.M. (1989) Eur. J. Biochem. 179, 241–248.
23 Maruyama, K. and MacLennan, D.H. (1988) Proc. Natl. Acad. Sci. USA 85, 3314–3318.
24 Clarke, D.M., Loo, T.W., Inesi, G. and MacLennan, D.H. (1989) Nature 339, 476–478.
25 Clarke, D.M., Maruyama, K., Loo, T.W., Leberer, E., Inesi, G. and MacLennan, D.H. (1989) J. Biol. Chem. 264, 11246–11251.
26 Green, N.M. (1989) Nature 339, 424–425.
27 Mitchinson, C., Wilderspin, A.F., Trinnaman, B.J. and Green, N.M. (1982) FEBS Lett. 146, 87–92.
28 Rizzolo, L.J. and Tanford, C. (1978) Biochemistry 17, 4049–4055.
29 Török, K., Trinnaman, B.J. and Green, N.M. (1988) Eur. J. Biochem. 173, 361–367.
30 Dux, L., Taylor, K.A., Ting-Beall, H.P. and Martonosi, A. (1985) J. Biol. Chem. 260, 11730–11743.
31 Dux, L., Papp, S. and Martonosi, A. (1985) J. Biol. Chem. 260, 13454–13458.
32 Deamer, D.W. (1973) J. Biol. Chem. 248, 5477–5485.
33 Ohnoki, S. and Martonosi, A. (1980) Comp. Biochem. Physiol. 65B, 181–189.
34 Dux, L., Lelkes, G., Hien, L.H. and Nemcsok, J. (1989) Comp. Biochem. Physiol. 92B, 263–270.
35 Wuytack, F., Kanmura, Y., Eggermont, J.A., Raeymaekers, L., Verbist, J., Hartweg, D., Gietzen, K. and Casteels, R. (1989) Biochem. J. 257, 117–123.
36 Dux, L. and Martonosi, A. (1983) J. Biol. Chem. 258, 10111–10115.
37 Gibbons, I.R., Lee-Eiford, A., Mocz, G., Phillipson, C.A., Tang, W.-J.Y. and Gibbons, B.H. (1987) J. Biol. Chem. 262, 2780–2786.
38 Tang, W.-J.Y. and Gibbons, I.R. (1987) J. Biol. Chem. 262, 17728–17734.
39 Mocz, G., Tang, W.-J. and Gibbons, I.R. (1988) J. Cell Biol. 106, 1607–1614.
40 Grammer, J.C. and Yount, R.G. (1987) Biophys. J. 51, 25a.
41 Mocz, G. (1989) Eur. J. Biochem. 179, 373–378.
42 Paschal, B.M., Shpetner, H.S. and Vallee, R.B. (1987) J. Cell Biol. 105, 1273–1282.
43 Lye, R.J., Porter, M.E., Scholey, J.M. and McIntosh, J.R. (1987) Cell 51, 309–318.
44 Chasteen, N.D. (1983) Struct. Bond. (Berlin) 53, 105–138.
45 Boyd, D.W. and Kustin, K. (1985) Adv. Inorg. Biochem. 6, 311–365.
46 Tracey, A.S. and Gresser, M.J. (1986) Proc. Natl. Acad. Sci. USA 83, 609–613.
47 Grammer, J.C., Cremo, C.R. and Yount, R.G. (1988) Biophys. J. 53, 237a.
48 Nakamura, H., Jilka, R.L., Boland, R. and Martonosi, A. (1976) J. Biol. Chem. 251, 5414–5423.
49 Varga, S., Mullner, N., Pikula, S., Papp, S., Varga, K. and Martonosi, A. (1986) J. Biol. Chem. 261, 13943–13956.
50 MacLennan, D.H. (1970) J. Biol. Chem. 245, 4508–4518.
51 Meissner, G., Conner, G.E. and Fleischer, S. (1973) Biochim. Biophys. Acta 298, 246–269.
52 Lowry, O.H., Rosebrough, N.J., Farr, A.L. and Randall, R.J. (1951) J. Biol. Chem. 193, 265–275.
53 Csermely, P., Martonosi, A., Levy, G.C. and Ejchart, A.J. (1985) Biochem. J. 230, 807–815.
54 Inesi, G. (1971) Science 171, 901–903.
55 Laemmli, U.K. (1970) Nature 227, 680–685.
56 King, L.E. and Morrison, M. (1976) Anal. Biochem. 71, 223–230.
57 Schibeci, A. and Martonosi, A. (1980) Anal. Biochem. 104, 335–342.
58 Johnson, D.T., Gautsch, J.W., Sportsman, J.R. and Elden, J.H. (1984) Gene Anal. Techn. 1, 3–8.
59 Goding, J.W. (1986) Monoclonal Antibodies: Principles and Practice. Production and Application of Monoclonal Antibodies in Cell Biology, Biochemistry andd Immunology, 2nd Edn., Academic Press, New York.
60 Zubrzycka-Gaarn, E., MacDonald, G., Phillips, L., Jørgensen, A.O. and MacLennan, D.H. (1984) J. Bioenerg. Biomembr. 16, 441–464.
61 Sarkadi, B., Enyedi, A., Penniston, J.T., Verma, A.K., Dux, L., Molnar, E. and Gardos, G. (1988) Biochim. Biophys. Acta 939, 40–46.
62 Seiler, S., Wegener, A.D., Whang, D.D., Hathaway, D.R. and Jones, L.R. (1984) J. Biol. Chem. 259, 8550–8557.
63 Borgen, O., Mahmoud, M.R. and Skauvik, I. (1977) Acta Chem. Scand. A31, 329–339.
64 Liochev, S.J., Ivancheva, E. and Russanov, E. (1988) Free Rad. Res. Commun. 4, 317–323.
65 Liochev, S. and Fridovich, I. (1988) Arch. Biochem. Biophys. 263, 299–304.
66 Liochev, S.J. and Fridovich, I. (1989) Free Rad. Biol. Med. 6, 617–622.
67 Markus, S., Priel, Z. and Chipman, D.M. (1986) Biochim. Biophys. Acta 874, 128–135.
68 Markus, S., Priel, Z. and Chipman, D.M. (1989) Biochemistry 28, 793–799.
69 Vanderkooi, J.M., Papp, S., Pikula, S. and Martonosi, A. (1988) Biochim. Biophys. Acta 957, 230–236.
70 Pick, U. and Karlish, S.J.D. (1980) Biochim. Biophys. Acta 626, 255–261.
71 Pick, U. and Karlish, S.J.D. (1982) J. Biol. Chem. 257, 6120–6126.
72 Pick, U. and Bassilian, S. (1981) FEBS Lett. 123, 127–130.
73 Pick, U. (1982) J. Biol. Chem. 257, 6111–6119.